A Discussion about a Start-up Procedure of a Doubly-Fed Induction Generator System

J. L. Da Silva*, R. G. de Oliveira*, S. R Silva*, B. Rabelo** and W. Hofmann**
*Federal University Of Minas Gerais/Electric Engineering Research and Development Center, Belo Horizonte, Brazil
**Dresden University of Technology/Dept. of Electrical Machines and Drives, Dresden, Germany

***Abstract*— The present work proposes a start-up procedure for a doubly-fed induction generator (DFIG) driven by a wind turbine. In the DFIG topology the stator is connected direct to the grid while the rotor is connected to a back-to-back converter. This structure requires some care during grid synchronization to avoid undesired overloads. The main goal of a start-up procedure is to reduce the stresses on the electrical and mechanical components during synchronization. In this work, it is achieved by equalization among the induced stator voltage, the voltage over the filter capacitor and the grid voltage. A phase-locked-loop (PLL) computes the grid voltage phase displacement required for the system control orientation and synchronization procedures.**

Previous to the starting-up, the output currents set-points of the grid-side converter and rotor-side converter are computed in order to produce the same grid voltage over the filter capacitors and on the stator terminals. The whole procedure is summarized in seven different steps: turbine acceleration by the pitch control, DC-link pre-charge; initialization of the filter current controllers; filter synchronization; DC-Link voltage adjust; rotor current controllers' initialization and stator synchronization. The proposed start-up procedure was tested in a 4 kW test bench and the description of each step as well as simulation and experimental results are presented throughout the paper.

***Index Terms*—Wind power generation, doubly-fed induction generator, synchronization, grid utility.**

I. Introduction

MANY governments are adopting new energy generation guidelines towards an ecologically sustainable society. This reflects in a continuous growth of wind power generation around the world in the last years. Among the wind generation concepts, the advantages of the adjustable speed are well known and can be summarized in reduction of torque pulsations (once wind gusts can be absorbed by the system), reduction of mechanical stresses and increase of energy production.

Nowadays, doubly-fed induction generators (DFIG) for wind turbines are widely used. The main advantage of the DFIG compared to the other adjustable speed generators is the fact that power electronics components only handle with a fraction of the generator power. This reduces the acquisition costs and the losses in power electronics devices. Finally, the quality of the generated power is also improved in terms of harmonic and voltage fluctuations [1], [2].

The DFIG topology is depicted in figure 1 and consists on the stator directly connected to the grid while the rotor circuit with its variable voltage and frequency requires a back-to-back converter for the grid connection. The converter allows the active power flow in two directions: from the grid to the rotor in sub-synchronous operation and from the rotor to the grid in over-synchronous mode. A LC-filter in the output of the grid-side converter is used for reducing the switching harmonics.

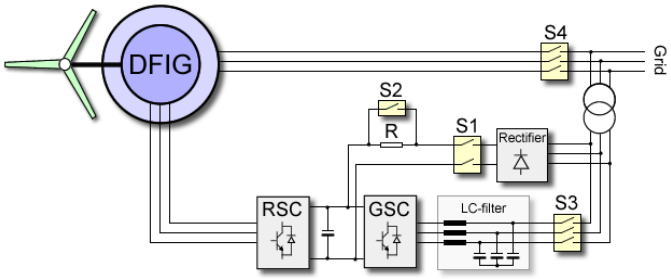

Figure 1. Scheme of the DFIG System

Since the size of the machines is increasing towards 5 MW, the stresses on the mechanical drive train and on the electrical circuits during connection to the supply cannot be neglected. Furthermore, the grid code requirements from the system operators on wind turbines foresee the limitation of the start-up currents on the net connecting point. Although, few papers have handled the starting-up procedure for the grid synchronization of a DFIG. In the related literature found, an induced stator voltage equal to the grid voltage is generated before the synchronization by adjusting the rotor flux [6], [7], [8], [9], [10]. This procedure performs a null current connection with a very low impact to the grid and the machine. The same principle is adopted in this paper. Although, a start-up procedure for the whole DFIG system is proposed in seven different steps described in a systematic way. Simulation and experimental results are also presented.

The proposed synchronization process can be carried out at any operational speed of the wind turbine rapidly and smoothly. This characteristic is very important not only for the start-up from zero speed but also during grid problems which lead to the generator disconnection. For example, voltage dips that exceed the duration specified by the grid code requirements. This causes tripping of protective relays, disconnecting the wind turbine system to the grid. A soft start-up allows the reclosing of the system as soon as the fault is cleared. Effectively, after the grid disconnection, the wind turbine can stay in a temporary running-up state. If the grid is not re-established after a certain time, the turbine is taken into a stop state [9]. Otherwise, the synchronization can be carried

out as fast as possible integrating the generator back to the grid.

The start-up procedure is characterized in seven different steps:

1. Turbine acceleration by the pitch control;
2. DC-link capacitor pre-charge;
3. Filter current controllers initialization;
4. Filter synchronization;
5. DC-link voltage adjust;
6. Rotor current controllers initialization;
7. Stator synchronization.

The basic conditions for both filter and stator synchronization are minimal deviations on the amplitude, frequency and phase angle between the grid and the voltages across the filter capacitor and on the stator terminals.

The process of DFIG disconnection from the grid is the reverse connecting process. The reduction of the wind speed will gradually unload the generator until minimum speed is reached. While approaching to the no load condition, the generator will be disconnected from the grid and the controllers can be switched off.

II. The DFIG System Control

A. Orientation

The 3-phase DFIG system can be mathematically transformed in a direct and quadrature axis system (*dq*-axis). These new axes compose a rotating reference frame. In this work, the voltage orientation is adopted, i.e. the *d*-axis is oriented to the direction of the grid voltage vector.

The frequency and phase displacement of the grid voltage are estimated by a phase-locked-loop (PLL) [3]. The correct estimation of these parameters is fundamental not only for the orientation but also for the quality of the grid connection. Thus, the PLL scheme depicted in figure 2 is adopted since it performs a robust way for calculating the grid angle.

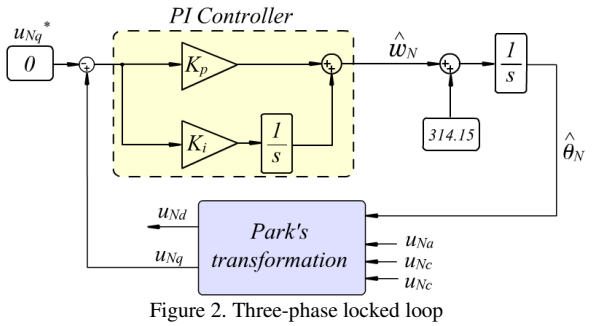

Figure 2. Three-phase locked loop

The stator voltage orientation is reached by setting the voltage *q*-component (u_{Nq}) to zero. The output of the PI controller gives the net angular frequency which is integrated in order to obtain the angle. This angle is fed-back and used for the *abc-to-dq* transformation. The result is used for the new error calculation. A specific value of frequency (ω_N = 314.15 for 50 Hz systems) is fed-forward to improve the overall tracking performance of the PLL.

The rotor components are oriented by the slip angle which is computed as the difference between the stator angle (given by the PLL) and the rotor angle (obtained from an encoder).

According to the orientation adopted, direct axis (*d*-components) represents active power and the quadrature axis (*q*-component), reactive power in the system.

B. Control Strategy

The control strategy is summarized in figure 3. It is accomplished by a cascaded structure in which the inner loops are the current ones. In the grid-side converter (GSC), two outer PI controllers are responsible for the DC-link voltage control (*d*-component) and the reactive power control (*q*-component). Likewise, in the rotor-side converter (RSC), the active component of the current receives the set-point from outer torque and speed controllers. The fixed set-point of the rotor reactive current defines the machine magnetization level through the rotor circuit. Space vector modulation (SVM) is used in order to generate the pulses for the IGBT gates [4]. The control strategy is very similar to the one first proposed by Peña et. al. [5].

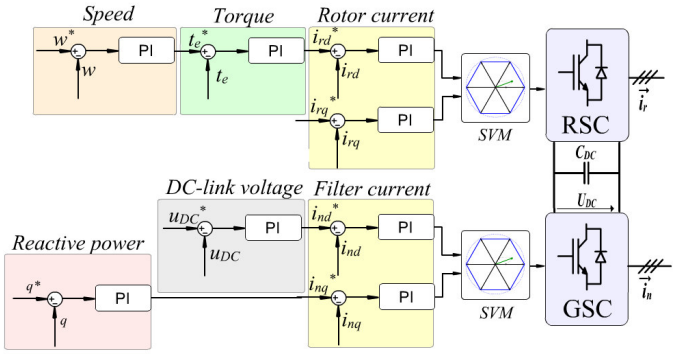

Figure 3. Control loops of the DFIG System

III. The DFIG System Model

A. The machine model

The generator's model is obtained from the classical equations of the induction machine. The stator and rotor voltages,

$$\underline{u}_s = R_s \underline{i}_s + \frac{d\underline{\psi}_s}{dt} + j\omega_s \underline{\psi}_s \quad (1)$$

$$\underline{u}_r = R_r \underline{i}_r + \frac{d\underline{\psi}_r}{dt} + j\omega_{slip} \underline{\psi}_r \quad (2)$$

and fluxes,

$$\underline{\psi}_s = L_s \underline{i}_s + L_m \underline{i}_r \quad (3)$$

$$\underline{\psi}_r = L_r \underline{i}_r + L_m \underline{i}_s \quad (4)$$

will be the basis for the mathematical manipulation of the equations. The electromagnetic torque is expressed as

$$T_e = \frac{3}{2} P_P \frac{L_m}{L_s} \Im \left\{ \underline{\Psi}_s \underline{i}_r^* \right\}. \quad (5)$$

Finally, the mechanical equation of the machine relates the electromagnetic and load torque with the rotor speed.

$$T_e - T_L = J \frac{d\omega_r}{dt} + B\omega_r \quad (6)$$

B. The DC-link model

The RSC and GSC are connected through a DC-link in a back-to-back topology. The power balance between the DC-link and the inverters' output is carried out. Thus, in order to obtain the current in the DC-link capacitor, a power distribution in used for calculating the total rotor (i_{rDC}) and filter (i_{nDC}) contribution for the DC-link current. Finally, the DC-link voltage (u_{DC}) is obtained according to the following expression,

$$u_{DC} = \frac{1}{C_{DC}} \int (i_{nDC} - i_{rDC}) dt + U_{DC0} \quad (7)$$

where C_{DC} is the DC link capacitance.

C. The LC-filter model

According to the voltage orientation adopted ($U_{Nq} = 0$) and considering that the voltage over the capacitor is the grid one (figure 1), GSC output voltages (u_{nd} and u_{nq}) are expressed as,

$$u_{nd} = R_f i_{nd} + L_f \frac{di_{nd}}{dt} - L_f \omega_N i_{nq} + U_{Nd} \quad (8)$$

$$u_{nq} = R_f i_{nq} + L_f \frac{di_{nq}}{dt} + L_f \omega_N i_{nd}. \quad (9)$$

IV. Simulation Results

A static stator connection is presented in figures 4 and 5. The fundamental component of the induced voltage over the stator and grid voltage present no amplitude, frequency and phase displacement deviation. A high frequency voltage noise is observed in the stator before the synchronization caused by the rotor currents ripple.

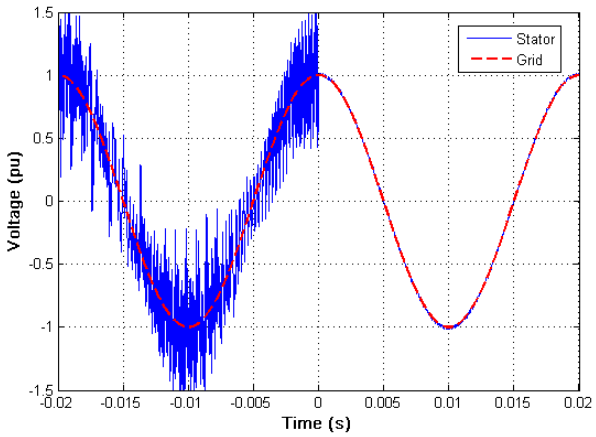

Figure 4. Stator connection

A satisfactory machine synchronization reflects in almost no impact in the grid and machine states. Figure 5 shows that after the grid connection is done (t = 0s), the speed is kept intact which could be translated into the torque absence. A very low oscillation can be observed in the rotor currents and the stator currents do not reach values higher than 0.01 pu.

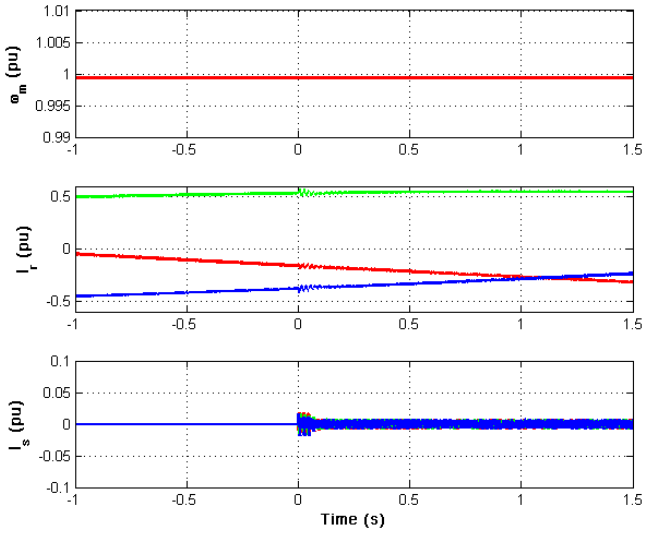

Figure 5. Synchronization impact in the machine speed and currents

Figure 6 shows three different amplitudes of the stator voltage (U_S) for the grid connection. It was simulated in the generator cut-in speed, i.e. 1050 rpm (70% of the synchronous speed). In the first case, U_S and the grid voltage (U_N) amplitude are the same before the synchronization. Very low currents flow in the stator (i_s). In the second test though, only 50% of the desired amplitude is induced ($U_S = 0.5U_N$). In this case, stator currents close to the nominal value appear. The worst case happens when no voltage is induced before the connection (U_N = 0). The current reaches amplitudes of two times the nominal current.

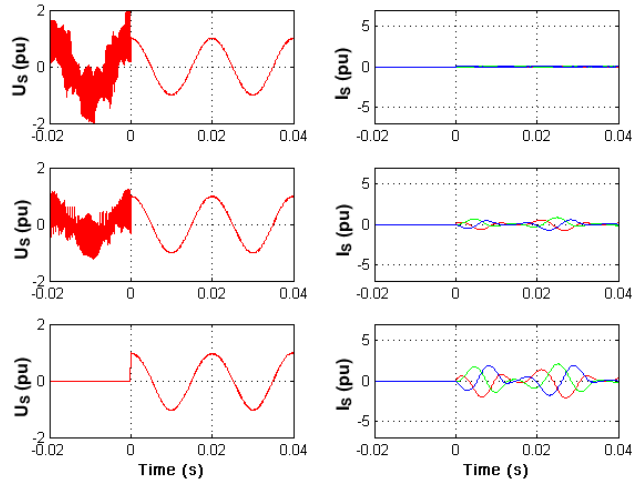

Figure 6. Stator voltage and currents during the synchronization with different amplitudes of the stator induced voltages

The phase displacement is more critical than amplitude

deviation as can be seen in figure 7. It shows the stator synchronization in three different situations: 0°, 90° and 180° of phase displacement of the stator voltage.

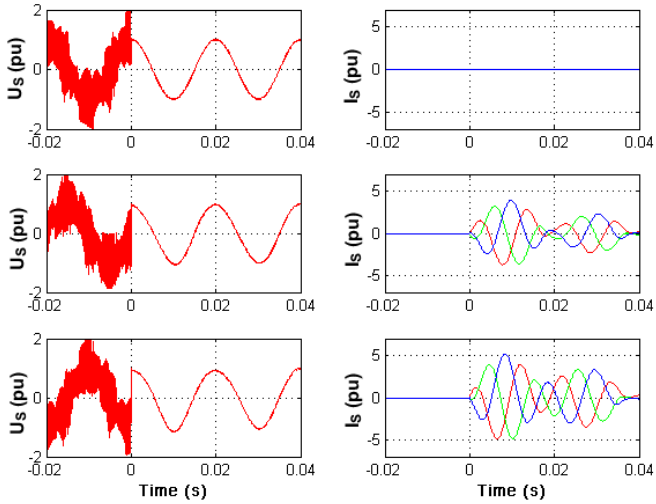

Figure 7. Stator voltage and currents during the synchronization with different phase displacements of stator induced voltages

The phase displacement causes higher transient currents than the amplitude errors. This transient currents can reach values up to five times the generator nominal value for the rotor speed of 1050 rpm.

Since a induced voltage in the stator with exactly the same grid voltage may not be achieved, the curves with the stator current transients for different errors may help in the definition of admissible $\underline{U_S}$ amplitude and phase displacement deviation. Thus, once defined the maximum synchronization currents, figure 8 allows the calculation of maximum admissible deviations in the induced voltage. For example, if the start-up current transient is defined to achieve values lower than 0.1 *pu,* the phase and amplitude error must keep values under 2%, i.e. 0.02 *pu* of voltage amplitude and 3.6° of phase displacement.

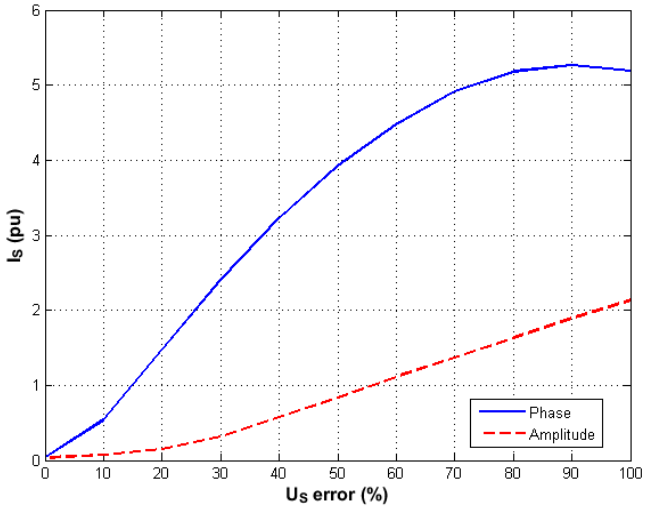

Figure 8. Stator current transients for U_N errors in phase and amplitude.

The same graph can be obtained for the filter synchronization. Figure 9 shows the error in the capacitor voltage (u_C) and the peak of the grid current (I_N) caused by the synchronization.

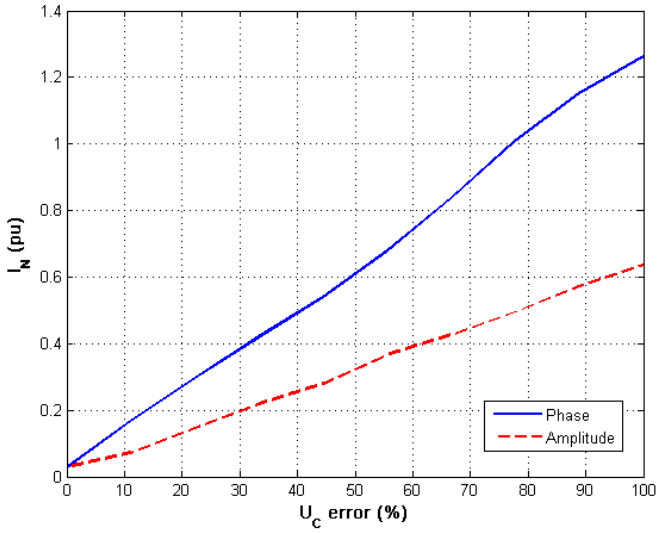

Figure 9. Grid current transient for u_C errors in phase and amplitude

V. Start-up Steps and Experimental Results

A. *Turbine acceleration by the pitch control*

The first step of the system start-up is the acceleration of the turbine made by the pitch control. The aerodynamic torque exerted by the turbine blades accelerates the generator shaft. The pitch angle is controlled in a way that maximum torque is produced and the acceleration process is shorter. This step is the longest due to the inertia of the involved masses and can be emulated using a first order transfer function modeling the mechanical system dynamics. During this process, steps 2 to 5 of the filter synchronization can take place. With the grid-side converter connected, step 6 can be carried out. After reaching the cut-in speed the generator can be synchronized.

B. *DC-link pre-charge*

The proposed strategy uses an uncontrolled diode rectifier for charging the DC-link. This process is made through a resistor which is responsible for defining the DC-link charge current and time constant. Another possibility would be using a three-phase resistor in series with the filter. The advantage of this approach is to eliminate the necessity of a rectifier. In the other hand, two other resistors would be necessary.

The use of the rectifier makes the GSC and the DFIG connection very similar. In both cases, the synchronization requires that the voltage across the filter capacitor and stator terminals are equal to the grid's. This is accomplished by controlling the *dq*-axis currents of the rotor and filter as will be presented later.

Figure 10 shows the DC-link charge through the power resistor. In moment (A) the switch S1 (figure 1) is closed charging the DC-link capacitors. When the voltage approaches its final value, the resistor (R) is by-passed with S2 (moment B).

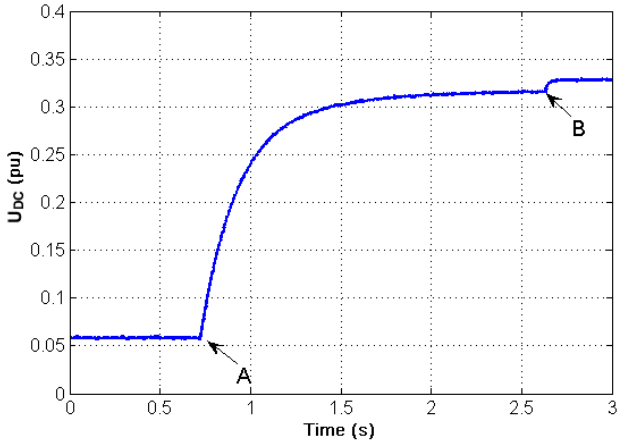

Figure 10. DC-link pre-charge

C. Filter current controllers initialization

After the DC-link is charged, the filter current controllers are initialized. The goal of this step is to generate the grid voltage across the filter capacitors. Both current set-points (i_{nd}* and i_{nq}*) are automatically calculated taking under consideration the filter impedance - $Z_f = R_f + j(X_l - X_c)$ - as expressed in the equations bellow,

$$i_{nd}^{*} = \mathrm{Re}\left\{\frac{(R_f + X_l)|i_n| + U_{Nd}}{Z_f}\right\} \quad (10)$$

$$i_{nq}^{*} = \mathrm{Im}\left\{\frac{(R_f + X_l)|i_n| + U_{Nd}}{Z_f}\right\} \quad (11)$$

where U_{Nd} is the grid voltage (given by the PLL).

D. Filter synchronization

The switch S3 is closed at the moment pointed with (A) in the figure 11.

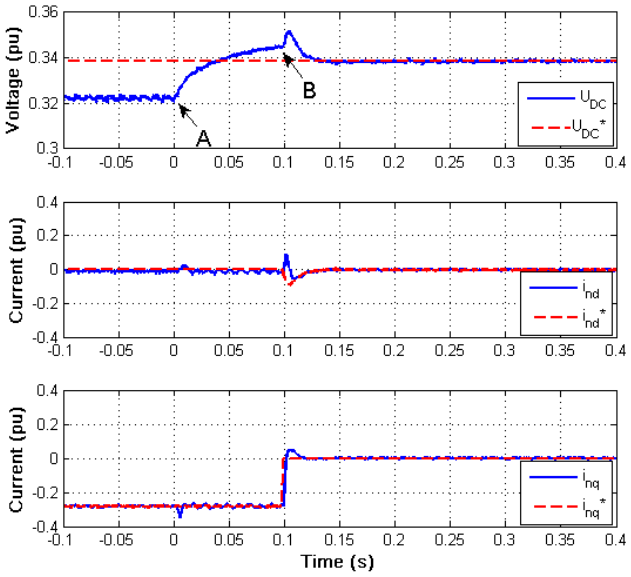

Figure 11. Filter synchronization

A small transient in the filter currents (i_{nd} and i_{nq}) can be observed during the synchronization followed by an increase of the DC-link voltage (U_{DC}). When this voltage deviation reaches a pre-defined threshold, the DC-link and reactive power controllers are automatically turned on at the moment pointed by (B) changing the *dq*-current set-points. The pre-charge circuit is then disconnected (S1 is opened) with no observed impact to the variables.

E. DC-Link voltage adjust

After the filter is connected to the grid, the DC-link voltage can be adjusted to the normal operational value. The voltage reference changes as a ramp making the process smooth as shown in figure 12.

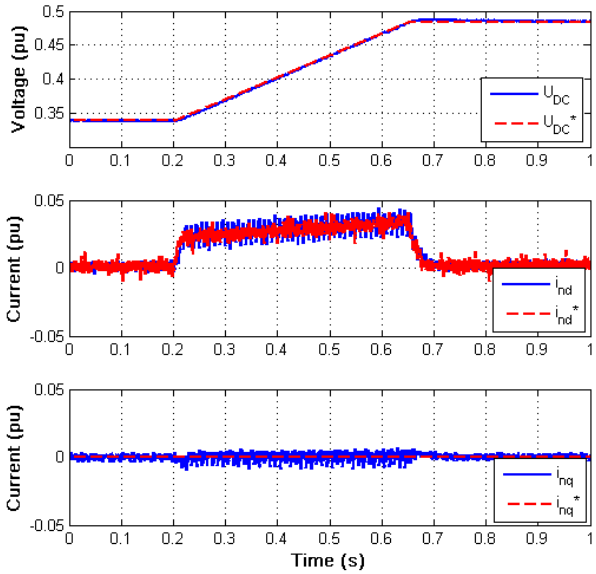

Figure 12. DC-link voltage adjust

F. Rotor current controllers initialization

The rotor current controllers are turned on in order to induce the voltage in the stator. The rotor currents set-points (i_{rd}* and i_{rq}*) are calculated based on the desired stator voltage (U_N) and the mathematical DFIG equations with opened stator as followed,

$$i'^{*}_{rd} = 0 \quad (12)$$

$$i'^{*}_{rq} = -\frac{u_{Nd}}{\omega_N L_m} \quad (13)$$

where u_{Nd}=|u_N| and u_{Nq}=0 (grid voltage orientation) and ω_N is the grid frequency.

G. Stator synchronization

The last step of the DFIG system start-up is the stator synchronization. It can be done at any machine speed. This is an important characteristic since no electromagnetic torque can be created with the opened stator, and the pitch control alone is the responsible for speed variations. A low impact for the DFIG can be observed in the behavior of the machine states when S4 is closed as shown in figure 13.

The synchronization bellow was carried out near to the synchronous speed. When the synchronization is carried out ($t=0s$) almost no changes are noticed in the speed and rotor currents (i_r). The stator currents (i_s) presented small transients. Figure 5 shows simulation results of grid connection in the same operating point. The comparison between the two graphs shows that the simulated and experimental results are very similar.

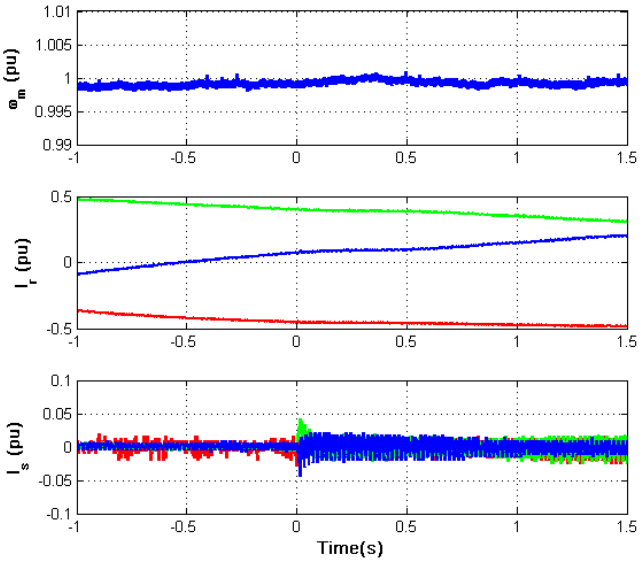

Figure 13. Synchronization of the DFIG

When the last start-up step is done, the torque and speed controllers are initialized in the maximum power point tracking mode and the system is fully integrated to the electrical network.

VI. Conclusion

This work discusses and presents a start-up procedure for a DFIG for wind turbine applications. The basic conditions for filter and stator synchronization are minimal deviations on the amplitude, frequency and phase angle between the grid and the voltages across the filter capacitor and on the stator terminals.

The complete synchronization process was explained in seven different steps: turbine acceleration by the pitch control; DC-link capacitor pre-charge; filter current controllers initialization; filter synchronization; DC-link voltage adjust; rotor current controllers initialization and stator synchronization. After these steps are accomplished, the maximum power tracking mode is initialized.

Simulation and experimental results were presented and showed that the start-up performs a smooth and fast connection with low impact to the machine and grid.

Appendix

System Parameters

Rated Power	P_{mec}	*4000 W*
Stator voltage	U_s	*380 V*
Stator current	I_s	*8.6 A*
Power factor	$cos\ \varphi$	*0.84*
Mechanical speed	N_m	*1440 rpm*
Rotor voltage	U_r	*160 V*
Rotor current	I_r	*15.5 A*
Stator resistance	R_s	*1.5* Ω
Rotor resistance	R_r	*0.9* Ω
Magnetizing inductance	L_m	*139 mH*
Stator inductance	L_s	*148 mH*
Rotor inductance	R_r	*141 mH*
Moment of Inertia	J	*0.045 kgm²*
Friction Coefficient	B	*0.00727 Nms*
Pair of poles	P_P	*2*
Filter inductance	L_f	*8 mH*
Filter Resistance	R_f	*0.5* Ω
Filter capacitance	R_f	*69 mF*

References

[1] B. Rabelo and W. Hofmann. Power flow optimisastion and grid integration of wind turbines with the doubly-fed induction generator. IEEE 36th Power Electronics Specialists Conference, pages 2930-2936, 2005.

[2] A. Peterson. Analysis, Modeling and Control of Doubly-Fed Induction Generators for Wind Turbines. PhD thesis, Chalmers University of Technology, Goeteborg, Sweden, 2005.

[3] S. Silva et. al. Pll structures for utility connected systems under distorted utility conditions. 32nd Annual Conference on IEEE Industrial Electronics, pages 2636-2641, 2006.

[4] J. Holtz. Pulsewidth modulation - a survey. 23rd Annual IEEE Power Electronics Specialists Conference, pages 11-18, 1992.

[5] R. Pena, J. Clare and G. Asher. Doubly fed induction generator using back-to-back PWM converters and its application to variable-speed wind-energy generation. IEE Proceeding in Electric Power Applications, pages 231-240, 1996.

[6] G. Yuan, J. Chai and Y. Li. Vector Control and Synchronization of Doubly Fed Induction Wind Generator System, IEEE 4th International Power Electronics and Motion Control Conference, pages 886-890, 2004.

[7] A.G. Abo-Khalil, D.-C. Lee, and S.-P. Ryu, Synchronization of DFIG Output Voltage to Utility Grid, European Power and Energy Systems, pages 1-6, 2006.

[8] X. Zhang, D. Xu, Y. Lang and H. Ma. Study on Stagewise Control of Connecting DFIG to the Grid, IEEE 5th International Power Electronics and Motion Control Conference, pages 1-5, 2006.

[9] S. A. Gomez and J. L. R. Amenedo. Grid synchronization of doubly fed induction generators using direct torque control, IEEE 28th Annual Conference of the Industrial Electronics Society, pages 3338-3343, 2002.

[10] K. P. Gokhale, D. W. Karraker and S. J. Heikkila. *Controller for a wound rotor slip ring induction machine,* United States patent, patent number 6448735, 2001.